Hindawi
Journal of Mathematics
Volume 2022, Article ID 9006361, 8 pages
https://doi.org/10.1155/2022/9006361

Research Article

Modeling Drug Concentration Level in Blood Using Fractional Differential Equation Based on Psi-Caputo Derivative

Muath Awadalla,[1] **Yves Yannick Yameni Noupoue**,[2] **Kinda Abu Asbeh**,[1] **and Noureddine Ghiloufi**[1,3]

[1]*Department of Mathematics and Statistics, College of Science, King Faisal University, Hafuf, Al Ahsa 31982, Saudi Arabia*
[2]*Université Catholique de Louvain, Louvain, La-Neuve, Belgium*
[3]*University of Gabes, Faculty of Sciences of Gabes, LR17ES11 Mathematics and Applications, 6072 Gabes, Tunisia*

Correspondence should be addressed to Muath Awadalla; mawadalla@kfu.edu.sa

Received 5 August 2022; Revised 1 September 2022; Accepted 5 September 2022; Published 28 September 2022

Academic Editor: Arzu Akbulut

This article studies a pharmacokinetics problem, which is the mathematical modeling of a drug concentration variation in human blood, starting from the injection time. Theories and applications of fractional calculus are the main tools through which we establish main results. The psi-Caputo fractional derivative plays a substantial role in the study. We prove the existence and uniqueness of the solution to the problem using the psi-Caputo fractional derivative. The application of the theoretical results on two data sets shows the following results. For the first data set, a psi-Caputo with the kernel $\psi = x + 1$ is the best approach as it yields a mean square error (MSE) of 0.04065. The second best is the simple fractional method whose MSE is 0.05814; finally, the classical approach is in the third position with an MSE of 0.07299. For the second data set, a psi-Caputo with the kernel $\psi = x + 1$ is the best approach as it yields an MSE of 0.03482. The second best is the simple fractional method whose MSE is 0.04116 and, finally, the classical approach with an MSE of 0.048640.

1. Introduction

To treat an infection from a human being or even from an animal, a suitable dose of medicine is substantial. Owing to the amount of the drug in the blood plasma decreasing with time, medicine must be given in multiple doses.

In phase I of clinical development, the time to achievement of steady state of a new regimen is routinely evaluated. The time to the achievability of the steady state is the time needed until the drug concentration is stable in the blood, i.e., does not display an increasing tendency by drug accumulation. If a drug is given at orderly dosing intervals, drug sediment from preceding doses is accumulated. Stabilization of the concentration occurs when the quantity of drug discarded during the dosing interval equals the amount that was given. In order to evaluate the time to achieve steady state, blood is sampled at a certain time point within each dosing interval see [1].

Following the drug concentrations at these time points [2] Jordan et al. proposed a model for the achievement of the steady state of the drug concentration in plasma. Authors of [3] proposed a model for the prediction of the "unbound brain-to-plasma" drug concentration ratio. Zhang et al. [4] studied the ratio of the drug concentration between tissues and plasma.

A simple and novel sensor was developed for the analysis of clinical doxorubicin (DOX) concentration based on the screen-printed electrode by evaluating the DOX concentration, see [5]. In [6] the authors evaluated the drug concentrations in postmortem blood samples where the value of concentrations slightly differs depending on the sample site. For more works on drug concentration in the blood, we refer the reader to the references [7–11].

Fractional calculus (F.C) helps to describe models and natural phenomena problems. Many researches have dedicated their work in this branch (see, e.g., previous studies [12–19]). The results obtained were significantly positive in

different fields of Medicine and Biology. The foundation of fractional calculus is laid on fractional integrals and derivatives. The efficiency of the fractional order model over the integer order is investigated by Bagley and Torvik [20]. Through fractional calculus, Djordjevic et al. [21] developed a rheological model of airway smooth muscle cells, which came as an alternative to the least square data fitting technique often used for this purpose. Recently, an application of fractional calculus to nanotechnology was proposed in [22]. These are just a few out of plenty examples of research works in which fractional calculus has proven its efficiency compared to existing classical approach.

This research article contributes to showing the power of mathematical modeling using fractional calculus. In particular, a class of fractional derivatives called ψ-Caputo, introduced by Almeida [23], has proven its efficiency in various applications including a recent study by Awadalla et al. [24]. A preliminary investigation on the topic of this study was carried out by us. The results of the said investigation are provided in this reference [25]. The main contribution of this work to the literature is the reduction or further minimization of the MSE in modeling the drug's concentration kinetics. The article starts with an introduction; then, some preliminaries of fractional calculus are covered. Elements of pharmacokinetics and the mathematical model of drug concentration in the blood are discussed in the third section. Main theoretical results are established in the fourth section followed by application examples in the fifth section. Finally, the last section provides concluding remarks on the overall study.

More generally, realization of this work was motivated by the aim to reduce modeling error in pharmacokinetics.

2. Preliminaries

This section is dedicated to preliminary tools that will enable a smooth study in upcoming sections. Indeed, F.C theories are built thanks to theorems, definitions, and lemmas. Similar to classical calculus, integrals and derivatives taken in the fractional sense are the foundation of F.C. Concerning the abovementioned sentences, selected definitions, theorems, and notations are discussed in this section. They play important roles in the rest of the paper.

Definition 1 (see [9]). The fractional integral of order $\xi > 0$ of a function $\mathscr{H} : [a, b] \longrightarrow \mathscr{R}_e$ taken in the Riemann-Liouville sense is defined as

$$\left({}_{\mathscr{R}\mathscr{L}}\mathscr{I}_{0^+}^{\xi}\mathscr{H} \right)(\varrho) = \frac{1}{\Gamma(\xi)} \int_0^{\rho} (\varrho - \vartheta)^{\xi - 1} \mathscr{H}(\vartheta) d\vartheta. \tag{1}$$

Equation (1) holds only if the right-hand side of the given integral is point-wise defined on $]0, +\infty[$. Note that the function Γ is the commonly-known gamma function, which is defined as follows: $\Gamma(u) = \int_0^{+\infty} \varrho^{u-1} e^{-\varrho} d\varrho$, $\forall u > 0$.

Definition 2 (see [9]). The Caputo derivative of order $\xi > 0$ of a function $\mathscr{H} : [a, b] \longrightarrow \mathscr{R}_e$ is defined as

$$\left({}_C\mathscr{D}^{\xi_{0^+}}\mathscr{H} \right)(\varrho) = \begin{cases} \dfrac{1}{\Gamma(n-\xi)} \displaystyle\int_0^{\varrho} (\varrho - \vartheta)^{n-\xi-1} \mathscr{H}^{(n)}(\vartheta) d\vartheta, & n-1 < \xi < n,\ \xi \in \mathscr{R}_e, \\ \mathscr{H}^{(n)}(\varrho), & \xi \in \mathbb{N}, \end{cases} \tag{2}$$

where $n = \lfloor \xi \rfloor + 1$, $\lfloor \xi \rfloor$ is the integer part of ξ.

Definition 3 (see [2]). Let $\xi > 0$, $\mathscr{H} \in \mathscr{L}^1[a, b]$ and $\psi \in \mathscr{C}^1[a, b]$ is selected to be an increasing function with $\psi'(x) \neq 0$, $\forall x \in [a, b]$; then, the notation $\mathscr{I}_{0^+}^{\xi,\psi}\mathscr{H}(\varrho)$ represents the fractional integral of $\mathscr{H}$ with respect to another function ψ, and it is defined by

$$\mathscr{I}_{0^+}^{\xi,\psi}\mathscr{H}(\varrho) = \frac{1}{\Gamma(\xi)} \int_0^{\rho} \psi'(\vartheta)(\psi(\varrho) - \psi(\vartheta))^{\xi - 1} \mathscr{H}(\vartheta) d\vartheta. \tag{3}$$

The idea of integrating a function definition is known as ψ – Caputo integral of the fractional integral is taken in the Caputo sense. This is used in the sequel for formulating the solution to the ψ – Caputo fractional model.

Definition 4 (see [2]). Let $\xi > 0$ and $\mathscr{H}, \psi \in \mathscr{C}^n[a, b]$ where ψ is an increasing function and $\psi'(x) \neq 0$, $\forall x \in [a, b]$. Then, $\left({}_C\mathscr{D}_{0^+}^{\xi,\psi}\mathscr{H} \right)(\varrho)$ denotes the fractional derivative of $\mathscr{H}$ with respect to ψ. ψ – Caputo if the fractional derivative is taken in the Caputo sense, and it is given by

$${}_{\mathscr{C}}\mathscr{D}_{0^+}^{\xi,\psi}\mathscr{H}(\varrho) = \frac{1}{\Gamma(n-\xi)} \int_0^{\varrho} \psi'(\vartheta)(\psi(\varrho) - \psi(\vartheta))^{n-\xi-1} \left(\frac{1}{\psi'(\vartheta)} \frac{d}{d\rho} \right)^n \mathscr{H}(\vartheta) d\vartheta. \tag{4}$$

Lemma 5 (see [2]). *Let $\xi > 0$ and n be a positive integer such that $\xi \in]n-1, n[$. For every $\mathscr{H}, \psi \in \mathscr{C}^n[a, b]$, we have*

$$\mathscr{I}_{0^+}^{\xi,\psi} \left({}_{\mathscr{C}}\mathscr{D}_{0^+}^{\xi,\psi}\mathscr{H} \right)(\varrho) = \mathscr{H}(\varrho) - \sum_{p=0}^{n-1} \frac{1}{p!} \left(\frac{1}{\psi'(\vartheta)} \frac{d}{d\varrho} \right)^p \mathscr{H}(0)(\psi(\varrho) - \psi(0))^p. \tag{5}$$

3. Pharmacokinetics and Drug Concentration Model

A brief definition and overview of pharmacokinetics are proposed in this section. To treat an infection from a human body, a suitable dose of medicine is substantial. Once a drug is administrated to an individual through intravenous injection, it has an initial concentration that decreases over time. The decrement appears as a result of metabolism and excretion. Pharmacokinetics is a branch of medicine that studies the dynamic (kinetics of drugs in a living body). Owing to the amount of the drug in the human body decreasing with time medicine must be given in multiple doses.

Two main streams of study exist in pharmacokinetics, the theoretical approach and the experimental approach.

The former approach focuses on the development of a pharmacokinetics (mathematical) model that predicts drug concentration levels in the blood over time. The latter method involves empirical development based on a biological sample, during which analytical methods for drugs and their metabolites are measured. In this case, it is required to have an adequate experimental setting for data collection and handling. This article focuses in the sequel on the development of a mathematical pharmacokinetics model. The entire process of absorption, distribution, metabolism, and elimination (ADME) of a drug is illustrated in the next figure as described in [26, 27].

Figure 1 represents the ADME process of a drug after it has been administrated to a human. The process is governed by a change in concentration over time. The change rate can be denoted by $\pm d(\text{concentration})/d\varrho$. More generally, let us denote by $\mathcal{Y}$ the drug concentration in the body; then, the mathematical model describing the rate change is given by

$$\frac{d\mathcal{Y}}{d\varrho} = -k\mathcal{Y}, \tag{6}$$

where k is a constant to be experimentally determined for each drug. If a patient is given an initial drug dose, $\mathcal{Y}_0$, then, the drug level in his body at any time is the solution of the differential equation defined by Eq. (6), that is,

$$\mathcal{Y}(\varrho) = \mathcal{Y}_0 e^{-k\varrho}. \tag{7}$$

The objective of this work is to prove the advantages of modeling drug concentration kinetics using fractional differential equations. Indeed, we will show empirically that modeling results using F.C are better than those obtained from classical calculus. The starting point is to build a fractional counterpart of Eq. (6). The said equation is built as follows

$${}_C\mathcal{D}_{0^+}^{\xi,\psi}\mathcal{Y}(\varrho) = -k\mathcal{Y}(\varrho),\ \xi \in]0,1[,\ \mathcal{Y}(0) = \mathcal{Y}_0. \tag{8}$$

or simply

$${}_C\mathcal{D}_{0^+}^{\xi,\psi}\mathcal{Y}(\varrho) = \mathcal{Q}(\varrho, \mathcal{Y}(\varrho)), \quad \xi \in]0,1[,\ \mathcal{Y}(0) = \mathcal{Y}_0. \tag{9}$$

The Lemma below is defined to introduce a general form of the solution to Eq. (9) representing drug concentration kinetics with initial condition.

Lemma 6. *Let us consider $\mathcal{Q}$, with the assumption that it is an integrable function, which is defined over $[0, \mathcal{T}]$. It follows that the solution of the fractional differential equation given by Eq. (9) has a general form which can be expressed by the following integral equation*

$$\mathcal{Y}(\varrho) = \mathcal{Y}_0 + \frac{1}{\Gamma(\xi)}\int_0^{\varrho}\psi'(\vartheta)(\psi(\varrho) - \psi(\vartheta))^{\xi-1}\mathcal{Q}(\vartheta, \mathcal{Y}(\vartheta))d\vartheta. \tag{10}$$

It is worth to highlight in Eq. (10) from Lemma 6 the presence of ψ-Caputo fractional integral.

Proof. Let us apply the operator $\mathcal{I}_{0^+}^{\xi,\psi}$ to both sides of Eq. (9) leads to $\mathcal{Y}(\varrho) - \mathcal{Y}_0 = \mathcal{I}_{0^+}^{\xi,\psi}\mathcal{Q}(\varrho, \mathcal{Y}(\varrho))$. □

Equation (10) can be rewritten in the following form

$$\mathcal{Y}(\varrho) = \mathcal{Y}_0 E_\xi\left[-k(\psi(\varrho) - \psi(0))^\xi\right]. \tag{11}$$

where $E_\xi(\varrho) = \sum_{n=0}^{+\infty}(\varrho^n/\Gamma(n\xi + 1))$, $\varrho \in \mathcal{R}_e$ is the Mittag-Leffler function.

In the application, Kernel functions are selected under the data distribution. There is not a steady rule for that. However, a linear kernel works well in many cases. Other commonly used kernel includes but is not limited to $\sqrt{u}$, $\log u$.

4. Main Result of Psi-Caputo Drug Concentration Model

This section aims to investigate theoretical study around Eq. (9). The final goal is to build prove of the existence and the uniqueness of a solution to Eq. (9).

Let $\mathcal{C}[0, \mathcal{T}]$ be the space of real valued functions that are continuous on $[0, \mathcal{T}]$ endowed with the norm of the uniform convergence: $\|\mathcal{Y}\|_\infty = \sup_{\varrho\in[0,\mathcal{T}]}|\mathcal{Y}(\varrho)|$ for every $\mathcal{Y} \in \mathcal{C}[0, \mathcal{T}]$. Then, $\Phi := (\mathcal{C}[0, \mathcal{T}], \|\bullet\|_\infty)$ is a Banach space.

An operator $\mathfrak{T} : \Phi \longrightarrow \Phi$ defined and attached to the problem introduced by Eq. (9) can be built as

$$\mathfrak{T}\mathcal{Y}(\varrho) = \mathcal{Y}_0 + \frac{1}{\Gamma(\xi)}\int_0^{\varrho}\psi'(\vartheta)(\psi(\varrho) - \psi(\vartheta))^{\xi-1}\mathcal{Q}(\vartheta, \mathcal{Y}(\vartheta))d\vartheta. \tag{12}$$

In what follows, the existence of a solution to Eq. (10) is proved followed by a proof of the uniqueness of the said solution. Before establishing the proof of the main results, let us first establish the following statements. Indeed, the statements are mathematical hypotheses that are used in sections dedicated to proofs.

$$(A_1)|\text{The function } \mathcal{Q} : [0, \mathcal{T}] \times \mathcal{R}_e \longrightarrow \mathcal{R}_e \text{ is continuous,} \tag{13}$$

$$(A_2)\left|\begin{array}{l}\text{There exists } \mathcal{L}_{\mathcal{Q}} > 0 \text{ such that,}\\ |\mathcal{Q}(\varrho, \mathcal{Y}_1) - \mathcal{Q}(\varrho, \mathcal{Y}_2)| \le \mathcal{L}_{\mathcal{Q}}|\mathcal{Y}_1 - \mathcal{Y}_2|, \quad \forall \varrho \in [0, \mathcal{T}],\end{array}\right. \tag{14}$$

$$(A_3)\left|\begin{array}{l}\text{There exists a function } \mathcal{H} \in \mathcal{C}([0, \mathcal{T}], \mathcal{R}_e^+) \text{ and a nondecreasing function,}\\ \chi : \mathcal{R}_e^+ \longrightarrow \mathcal{R}_e^+ \text{ such that } |\mathcal{Q}(\varrho, \mathcal{Y})| \le \mathcal{H}(\varrho)\chi(|\mathcal{Y}|), \quad \forall(\varrho, \mathcal{Y}) \in [0, \mathcal{T}] \times \mathcal{R}_e.\end{array}\right. \tag{15}$$

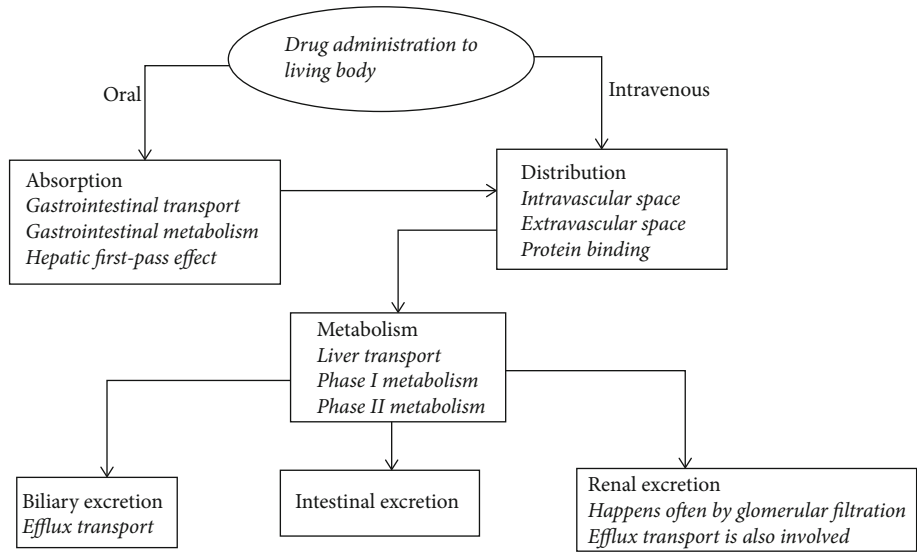

Figure 1: ADME process.

$$(A_4)\left|\begin{array}{l}\text{There exists a constant } W>0 \text{ such that,}\\ \dfrac{W}{|\mathcal{Y}_0|+\|\mathcal{H}\|_\infty\chi(\lambda)\left((1/\Gamma(\xi+1))(\psi(\mathcal{T})-\psi(0))^{\xi}\right)}>1.\end{array}\right. \tag{16}$$

Existence of at least one solution to the problem Eq. (9) is proved in the theorem below

Theorem 7. *Let us assume that the three conditions* (A_1), (A_3), *and* (A_4) *hold. Then, there exists at least one solution to Eq. (9). The said solution is in the interval* $[0,\mathcal{T}]$.

Proof. The proof of heorem 7 will be divided into several steps. The first step consists of showing that the operator $\mathfrak{T}:\Phi\longrightarrow\Phi$ maps bounded sets of Φ into bounded sets of Φ. Let $\mathfrak{B}_\lambda=\{\mathcal{Y}\in\Phi;\|\mathcal{Y}\|_\infty\le\lambda\}$ be a bounded set of Φ. Then

$$\begin{aligned}|\mathfrak{T}\mathcal{Y}(\varrho)|&\le|\mathcal{Y}_0|+\frac{1}{\Gamma(\xi)}\int_0^{\varrho}\psi'(\vartheta)(\psi(\varrho)-\psi(\vartheta))^{\xi-1}|\mathbb{Q}(\vartheta,\mathcal{Y}(\vartheta))|d\vartheta\\&\le|\mathcal{Y}_0|+\frac{1}{\Gamma(\xi)}\int_0^{\varrho}\psi'(\vartheta)(\psi(\varrho)-\psi(\vartheta))^{\xi-1}\mathcal{H}(\vartheta)\chi(\|\mathcal{Y}\|_\infty)d\vartheta\\&\le|\mathcal{Y}_0|+\|\mathcal{H}\|_\infty\chi(\|\mathcal{Y}\|_\infty)\frac{1}{\Gamma(\xi+1)}(\psi(\varrho)-\psi(0))^{\xi}.\end{aligned} \tag{17}$$

□

Applying the supremum on t on both sides of Eq. (17) leads to

$$\|\mathfrak{T}\mathcal{Y}\|_\infty\le|\mathcal{Y}_0|+\|\mathcal{H}\|_\infty\chi(\lambda)\frac{1}{\Gamma(\xi+1)}(\psi(\mathcal{T})-\psi(0))^{\xi}. \tag{18}$$

The second step of this proof is to show that the operator $\mathfrak{T}:\Phi\longrightarrow\Phi$ maps bounded sets of Φ into equi-continuous sets of Φ.

Let $\varrho_1,\varrho_2\in[0,\mathcal{T}]$ with $\varrho_1<\varrho_2$ and $\mathcal{Y}\in\mathfrak{B}_\lambda$. The relation below holds as results of the assumptions $(A1)$-$(A4)$

$$\begin{aligned}&|\mathfrak{T}\mathcal{Y}(\varrho_2)-\mathfrak{T}\mathcal{Y}(\varrho_1)|\\&\le\chi(\|\mathcal{Y}\|_\infty)\left|\frac{1}{\Gamma(\xi)}\int_0^{\varrho_1}\psi'(\vartheta)\left[(\psi(\varrho_2)-\psi(\vartheta))^{\xi-1}\right.\right.\\&\quad\left.-(\psi(\varrho_1)-\psi(\vartheta))^{\xi-1}\right]\mathcal{H}(\vartheta)d\vartheta\\&\quad\left.+\frac{1}{\Gamma(\xi)}\int_{\varrho_1}^{\varrho_2}\psi'(\vartheta)(\psi(\varrho_2)-\psi(\vartheta))^{\xi-1}\mathcal{H}(\vartheta)d\vartheta\right|.\end{aligned} \tag{19}$$

The right-hand side of Eq. (19) tends to zero as $\varrho_1\longrightarrow\varrho_2$. That is $|\mathfrak{T}\mathcal{Y}(\varrho_2)-\mathfrak{T}\mathcal{Y}(\varrho_1)|\longrightarrow0$ as $\varrho_1\longrightarrow\varrho_2$.

It is worth observing that the right hand part of Eq. (19) does not depend on $\mathcal{Y}\in\mathfrak{B}_\lambda$, this implies by Arzela-Ascoli theorem that $\mathfrak{T}(\mathfrak{B}_\lambda)$ is completely continuous.

The third step of the proof requires a last intermediate step to complete the assumptions of the Leray-Schauder nonlinear alternative theorem. This consists of showing the boundedness of the set of all solutions to equation $\mathcal{Y}=\delta\mathfrak{T}(\mathcal{Y})$. Assume that $\mathcal{Y}$ is a solution Eq. (9), then, it follows from Eq. (10) that

$$\begin{aligned}|\mathcal{Y}(\varrho)|=|\delta\mathfrak{T}(\mathcal{Y})(\varrho)|&\le\delta\left(|\mathcal{Y}_0|+\|\mathcal{H}\|_\infty\chi(\lambda)\frac{1}{\Gamma(\xi+1)}(\psi(\mathcal{T})-\psi(0))^{\xi}\right)\\&\le|\mathcal{Y}_0|+\|\mathcal{H}\|_\infty\chi(\lambda)\frac{1}{\Gamma(\xi+1)}(\psi(\mathcal{T})-\psi(0))^{\xi}.\end{aligned} \tag{20}$$

Inverting both sides of Eq. (20) and dividing them by R.H.S of Eq. (20) leads to the following relation

$$\frac{\|\mathcal{Y}\|_\infty}{|\mathcal{Y}_0|+\|\mathcal{H}\|_\infty\chi(\lambda)(1/\Gamma(\xi+1))(\psi(\mathcal{T})-\psi(0))^{\xi}}\le1. \tag{21}$$

Recalling (A_4), there exists a constant $W > 0$, which is indeed such that $W \neq \mathcal{Y}$. Moreover, let us construct the set $\Omega = \{\mathcal{Y} \in \Phi; \|\mathcal{Y}\|_\infty < W\}$. It is obvious that the operator $\mathfrak{T} : \bar{\Omega} \longrightarrow \Phi$ is continuous and completely continuous. Based on the constructed Ω, there exists $\mathcal{Y} \in \partial\Omega$ such that $\mathcal{Y}\delta\mathfrak{T}(\mathcal{Y})$ for some $\delta \in]0, 1[$. Consequently, by the nonlinear alternative of Leray-Schauder type, we deduce that $\mathfrak{T}$ has a fixed point $\mathcal{Y} \in \bar{\Omega}$ which is a solution to the problem defined by Eq. (10).

Theorem 8. *Let us assume that conditions (A_1) and (A_2) hold. Moreover, if the condition*

$$\frac{\mathcal{L}_{\mathcal{Y}}}{\Gamma(\xi+1)}(\psi(\mathcal{T}) - \psi(0))^{\xi} < 1, \tag{22}$$

holds; then, the problem defined by Eq. (9) has a solution which is unique. The said solution belongs to the interval $[0, \mathcal{T}]$.

Proof. Let us consider the operator $\mathfrak{T}$ defined in Eq. (12). Let us also define a ball

$$\mathfrak{B}_\lambda := \{\mathcal{Y} \in \Phi; \|\mathcal{Y}\|_\infty \leq \varepsilon\} \text{ with } \varepsilon \geq \frac{|\mathcal{Y}_0| + (\mathcal{M}_{\mathcal{Q}}/\Gamma(\xi+1))(\psi(\mathcal{T}) - \psi(0))^{\xi}}{1 - (\mathcal{L}_{\mathcal{Y}}/\Gamma(\xi+1))(\psi(\mathcal{T}) - \psi(0))^{\xi}}, \tag{23}$$

where $\mathcal{M}_{\mathcal{Q}} := \sup_{0\leq\varrho\leq\mathcal{T}}|\mathcal{Q}(\varrho, 0)|$. □

First, let us show that $\mathfrak{T}\mathfrak{B}_\varepsilon \subset \mathfrak{B}_\varepsilon$. For any $\mathcal{Y} \in \mathfrak{B}_\varepsilon$, $\rho \in [0, \mathcal{T}]$, and using Eq. (12), we have the following relation

$$|\mathfrak{T}\mathcal{Y}(\varrho)| \leq |\mathcal{Y}_0| + \frac{1}{\Gamma(\xi)}\int_0^{\varrho}\psi'(\vartheta)(\psi(\varrho) - \psi(\vartheta))^{\xi-1}|\mathcal{Q}(\vartheta, \mathcal{Y}(\vartheta))|d\vartheta. \tag{24}$$

On the other hand,

$$\begin{aligned}|\mathcal{Q}(\vartheta, \mathcal{Y}(\vartheta))| &\leq |\mathcal{Q}(\vartheta, \mathcal{Y}(\vartheta)) - \mathcal{Q}(\vartheta, 0)| + |\mathcal{Q}(\vartheta, 0)| \\ &\leq \mathcal{L}_{\mathcal{Q}}\|\mathcal{Y}\|_\infty + \mathcal{M}_{\mathcal{Q}} \leq \mathcal{L}_{\mathcal{Q}}\varepsilon + \mathcal{M}_{\mathcal{Q}}.\end{aligned} \tag{25}$$

Substituting the appropriate fragment of equation in Eq. (24) by Eq. (25) implies a new relation which is given by

$$\|\mathfrak{T}\mathcal{Y}\|_\infty \leq |\mathcal{Y}_0| + \frac{1}{\Gamma(\xi+1)}(\psi(\mathcal{T}) - \psi(0))^{\xi}(\mathcal{L}_{\mathcal{Q}}\varepsilon + \mathcal{M}_{\mathcal{Q}}) \leq \varepsilon. \tag{26}$$

Equation (26) is sufficient to conclude that $\mathfrak{T}\mathfrak{B}_\varepsilon \subset \mathfrak{B}_\varepsilon$.

The second step of the proof is to show that the considered operator is a contraction mapping. For every $\mathcal{Y}_1$, $\mathcal{Y}_2 \in \Phi$, the following relation holds.

$$\begin{aligned}|\mathfrak{T}\mathcal{Y}_1(\varrho) - \mathfrak{T}\mathcal{Y}_1(\varrho)| &\leq \frac{1}{\Gamma(\xi)}\int_0^{\varrho}\psi'(\vartheta)(\psi(\varrho) - \psi(\vartheta))^{\xi-1}|\mathcal{Q}(\vartheta, \mathcal{Y}_1(\vartheta)) \\ &\quad - \mathcal{Q}(\vartheta, \mathcal{Y}_2(\vartheta))|d\vartheta \\ &\leq \left(\frac{1}{\Gamma(\xi)}\int_0^{\varrho}\psi'(\vartheta)(\psi(\varrho) - \psi(\vartheta))^{\xi-1}d\vartheta\right)\mathcal{L}_{\mathcal{Q}}\|\mathcal{Y}_1 - \mathcal{Y}_2\|_\infty \\ &\leq \left(\frac{\mathcal{L}_{\mathcal{Q}}}{\Gamma(\xi+1)}(\psi(\mathcal{T}) - \psi(0))^{\xi}\right)\|\mathcal{Y}_1 - \mathcal{Y}_2\|_\infty.\end{aligned} \tag{27}$$

From Eq. (27), we deduce that $\mathfrak{T}$ is a contraction. By the Banach contraction mapping theorem, the problem defined by Eq. (9) has a unique solution. The said solution belongs to the interval $[0, \mathcal{T}]$.

5. Application Example

In this section, application examples are provided to support the theoretical work developed above. Data set obtained from real-life experiment were used. The classical method, simple fractional method, and kernel fractional method were used to fit the data set. Finally, a comparison of results is done to support theoretical findings.

5.1. First Experimental Data Set. This data set was retrieved from [28]. The author carried out an experiment in which he measured a drug concentration in (mg/L) over 6 hours of an antibiotic. A single dose of the said antibiotic was administered intravenously to a 50-kilogram woman. The dose level was 20 mg/kg. A scatter plot of the concentration data over time shows a decay. Three deterministic approaches were used to fit the data set. The first approach is what is referred to as the classical approach, in which the general solution is defined by Eq. (7). The second and third approaches are fractional differential method and kernel fractional differential method, respectively, which general solutions are given by Eq. (11), respectively, with $\psi(x) = x$, trivial kernel, and $\psi(x) \neq x$, pure kernel. The selected pure kernel here is linear $\psi(x) = x + 1$. It was observed empirically that using any linear kernel $\psi(x) = x + a$, with $a \neq 0$, would produce a similar result to the case where $\psi(x) = x + 1$ is used.

Table 1 summarises one hand best estimates of the parameters for both classical and fractional approaches. On the other hand, it displays the MSE of each method. It is observed that the fractional kernel method with $\psi(x) = x + 1$ performed the best, followed by the fractional method with $\psi(x) = x$ and lastly the classical method. It is worth highlighting consistency in the results. Indeed, the solution to the classical approach is a first order differential equation; therefore, one would expect the solution to its fractional counterparts to be such that $\xi \in (0, 1) \cup (1, 2)$.

Figure 2 is the graph of the original data set, the fitted line is obtained from the classical model, and the fitted line is obtained from the fractional method with $\psi(x) = x$. Both fitted lines overlap over each other at the beginning of the plot but show a difference toward the end. The fractional

Table 1: Results of the first experiment.

parameter / Method	k	ξ	MSE
Classical method	0.53355		0.07299
Fractional with $\psi(x) = x$	0.51749	1.13327	0.05814
Fractional with $\psi(x) = x + 1$	0.49621	1.11080	0.04065

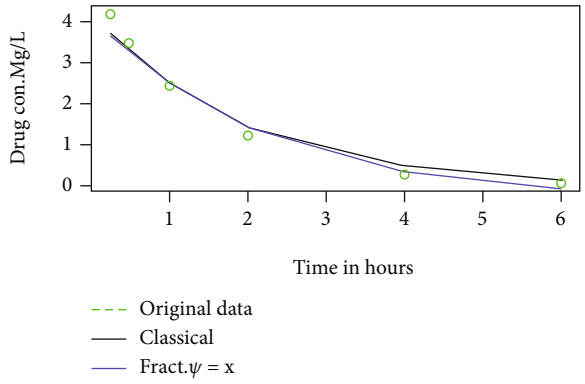

Figure 2: Original, classical, and fractional. $\psi(x) = x$.

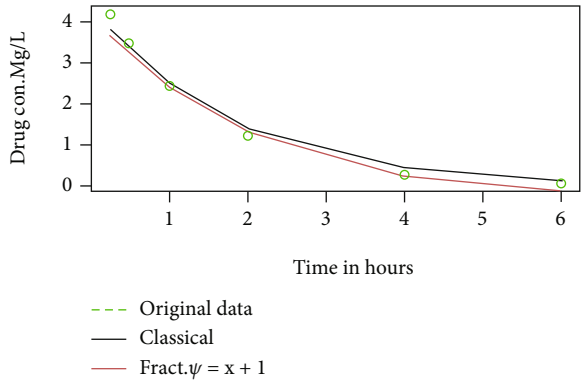

Figure 3: Original, classical, and fractional. $\psi(x) = x + 1$.

Table 2: Results of the second experiment.

parameter / Method	k	ξ	MSE
Classical method	0.34785		0.048640
Fractional with $\psi(x) = x$	0.34714	1.00456	0.04116
Fractional with $\psi(x) = x + 1$	0.34590	1.00360	0.03482

method with $\psi(x) = x$ seems to be closer to the true data. MSE in Table 1 is an evidence.

Figure 3 is the graph of the original data set, the fitted line is obtained from the classical model, and the fitted line is obtained from the fractional method with $\psi(x) = x + 1$. Similar to Figure 2, a close look at the figure reveals that the fractional method with $\psi(x) = x + 1$ does the job better than the classical method. Moreover, recalling Figures 2 and 3 as well as Table 1, the ordinal classification (first : fractional method with $\psi(x) = x + 1$; second : fractional method with $\psi(x) = x$; and third : classical method) of the three methods used in this work becomes explicit.

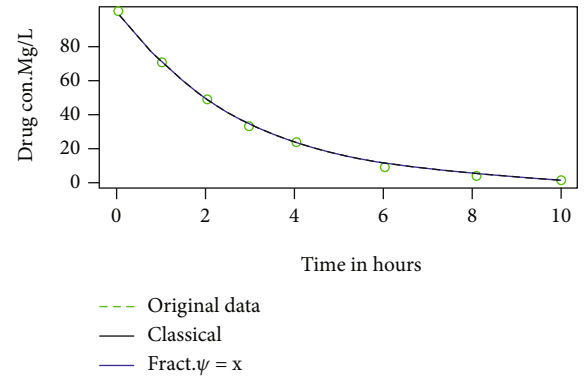

Figure 4: Original, classical, and fract. $\psi(x) = x$.

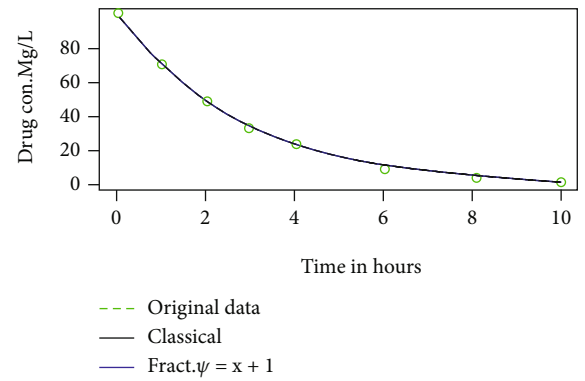

Figure 5: Original, classical, and fract. $\psi(x) = x + 1$.

5.2. Second Experimental Data Set. In this experiment, a newly developed drug was administrated to a patient. The administration was done through an IV injection. A sample of blood was taken regularly, and the drug plasma concentration was determined. The data set was retrieved from [29].

Similar experimental procedures to those from the first example are used. The best values of parameters as well as MSE of each method are consigned in the table below.

Table 2 summarises and displays the results of the second experiment. It is observed that the fractional kernel method with $\psi(x) = x + 1$ performed the best, followed by the fractional method with $\psi(x) = x$ and lastly the classical method. Moreover, the fractional order of derivatives is always such that $\xi \in (0, 1) \cup (1, 2)$, proving that the results are in line with the first-order differential equation. Hence, the results are consistent.

Figure 4 displays the original data, the classical solution, and the fractional with the kernel $\psi(x) = x$. The results in Table 2 are reflected by the fact that the fractional approach fits the original data points better than the classical approach does.

Figure 5 is the graph of the original data set, the fitted line is obtained from the classical model, and the fitted line is obtained from the fractional method with $\psi(x) = x + 1$. A close check of the figure reveals that the fractional method with $\psi(x) = x + 1$ does the job better than the classical method.

6. Conclusion and Future Work

In this work, we studied the ψ-Caputo type of fractional differential equation. This derivative is the fractional analog of the so-called $(\text{fog})'$ derivative in classical calculus. The existence and uniqueness of the proposed method were discussed before the application examples. Experiment results show that the ψ-Caputo method which uses a pure kernel function performed the best, followed by a simple fractional approach and finally the classical method. The fractional order of derivative that allows to best fit the data is always such that $\xi \in (0, 1) \cup (1, 2)$, which is in line with the setup of the studied problem since the classical approach solution is a first-order differential equation. The experimental section has revealed the following results:

For the first data set, a psi-Caputo with the kernel $\psi = x + 1$ is the best approach as it yields a mean square error (MSE) of 0.04065. The second best is the simple fractional method whose MSE is 0.05814; finally, the classical approach is in the third position with an MSE of 0.07299.

For the second data set, a psi-Caputo with the kernel $\psi = x + 1$ is the best approach as it yields an MSE of 0.03482 . The second best is the simple fractional method whose MSE is 0.04116 and, finally, the classical approach with an MSE of 0.048640.

In future works, we aim to investigate if the obtained results hold for all or most of existing fractional derivatives. We may also study properties that can help in the selection of a suitable kernel function. In the current study, the selection ψ function was done randomly, on a try and error basis, until we found out that a family of linear functions could well do the job.

Data Availability

The data set used in application section is available through the url provided in [27].

Conflicts of Interest

The authors declare that they have no competing interests.

Authors' Contributions

Each of the authors, M.A, Y.Y.Y, K.A, and N.G., contributed to each part of this work equally and read and approved the final version of the manuscript.

Acknowledgments

This article was funded by the Deanship of Scientific Research, King Faisal University (KFU), Ahsa, Saudi Arabia. The authors, therefore, acknowledge technical and financial support under NASHER track with a grant number (NA00080) of DSR at KFU.

References

[1] M. Rowland and T. N. Tozer, *Clinical Pharmacokinetics: Concepts and Applications*, Williams and Wilkins, Baltimore, 1995.

[2] P. Jordan, H. Brunschwig, and E. Luedin, "Modeling attainment of steady state of drug concentration in plasma by means of a Bayesian approach using MCMC methods," *Pharmaceutical Statistics*, vol. 7, no. 1, pp. 36–41, 2008.

[3] S. Varadharajan, S. Winiwarter, L. Carlsson et al., "Exploring _in silico_ prediction of the unbound brain-to-plasma drug concentration ratio: model validation, renewal, and interpretation," *Journal of Pharmaceutical Sciences*, vol. 104, no. 3, pp. 1197–1206, 2015.

[4] D. Zhang, C. E. C. A. Hop, G. Patilea-Vrana et al., "Drug concentration asymmetry in tissues and plasma for small molecule-related therapeutic modalities," *Drug Metabolism and Disposition*, vol. 47, no. 10, pp. 1122–1135, 2019.

[5] A. Peng, H. Xu, C. Luo, and H. Ding, "Application of a disposable doxorubicin sensor for direct determination of clinical drug concentration in patient blood," *International Journal of Electrochemical Science*, vol. 11, pp. 6266–6278, 2016.

[6] B. Zilg, G. Thelander, B. Giebe, and H. Druid, "Postmortem blood sampling–comparison of drug concentrations at different sample sites," *Forensic Science International*, vol. 278, pp. 296–303, 2017.

[7] M. Gibaldi, R. Nagashima, and G. Levy, "Relationship between drug concentration in plasma or serum and amount of drug in the body," *Journal of Pharmaceutical Sciences*, vol. 58, no. 2, pp. 193–197, 1969.

[8] P. J. McNamara, G. Levy, and M. Gibaldi, "Effect of plasma protein and tissue binding on the time course of drug concentration in plasma," *Journal of Pharmacokinetics and Biopharmaceutics*, vol. 7, no. 2, pp. 195–206, 1979.

[9] R. E. Bullingham, H. J. McQuay, E. J. Porter, M. C. Allen, and R. A. Moore, "Sublingual buprenorphine used postoperatively: ten hour plasma drug concentration analysis," *British Journal of Clinical Pharmacology*, vol. 13, no. 5, pp. 665–673, 1982.

[10] T. Uchimura, M. Kato, T. Saito, and H. Kinoshita, "Prediction of human blood-to-plasma drug concentration ratio," *Biopharmaceutics & Drug Disposition*, vol. 31, no. 5-6, pp. 286–297, 2010.

[11] S. Notari, C. Mancone, M. Sergi et al., "Determination of antituberculosis drug concentration in human plasma by MALDI-TOF/TOF," *IUBMB Life*, vol. 62, no. 5, pp. 387–393, 2010.

[12] T. K. H. Vu, D. T. Hung, V. I. Wheaton, and S. R. Coughlin, "Molecular cloning of a functional thrombin receptor reveals a novel proteolytic mechanism of receptor activation," *Cell*, vol. 64, no. 6, pp. 1057–1068, 1991.

[13] D. Baleanu, Z. B. Güvenç, and J. T. Machado, *New Trends in Nanotechnology and Fractional Calculus Applications*, Springer, New York, 2010.

[14] A. A. Kilbas, H. M. Srivastava, and J. J. Trujillo, *Theory and Applications of Fractional Differential Equations (Vol. 204)*, Elsevier, 2006.

[15] A. Atangana and B. S. T. Alkahtani, "Analysis of the Keller-Segel model with a fractional derivative without singular kernel," *Entropy*, vol. 17, no. 12, pp. 4439–4453, 2015.

[16] Z. J. Fu, W. Chen, and H. T. Yang, "Boundary particle method for Laplace transformed time fractional diffusion equations," *Journal of Computational Physics*, vol. 235, pp. 52–66, 2013.

[17] R. I. T. U. Agarwal, S. O. N. A. L. Jain, and R. P. Agarwal, "Mathematical modeling and analysis of dynamics of cytosolic calcium ion in astrocytes using fractional calculus," *Journal of Fractional Calculus and Applications*, vol. 9, no. 2, pp. 1–12, 2018.

[18] T. F. Wiesner, B. C. Berk, and R. M. Nerem, "A mathematical model of cytosolic calcium dynamics in human umbilical vein endothelial cells," *American Journal of Physiology-Cell Physiology*, vol. 270, no. 5, pp. C1556–C1569, 1996.

[19] L. Lenoci, M. Duvernay, S. Satchell, E. DiBenedetto, and H. E. Hamm, "Mathematical model of PAR1-mediated activation of human platelets," *Molecular BioSystems*, vol. 7, no. 4, pp. 1129–1137, 2011.

[20] R. L. Bagley and P. J. Torvik, "A theoretical basis for the application of fractional calculus to viscoelasticity," *Journal of Rheology*, vol. 27, no. 3, pp. 201–210, 1983.

[21] V. D. Djordjević, J. Jarić, B. Fabry, J. J. Fredberg, and D. Stamenović, "Fractional derivatives embody essential features of cell rheological behavior," *Annals of Biomedical Engineering*, vol. 31, no. 6, pp. 692–699, 2003.

[22] D. Kumar, J. Singh, and D. Baleanu, "Numerical computation of a fractional model of differential-difference equation," *Journal of Computational and Nonlinear Dynamics*, vol. 11, no. 6, 2016.

[23] R. Almeida, "A Caputo fractional derivative of a function with respect to another function," *Communications in Nonlinear Science and Numerical Simulation*, vol. 44, pp. 460–481, 2017.

[24] M. Awadalla, Y. Y. Yameni Noupoue, and K. Abuasbeh, "Psi-Caputo logistic population growth model," *Journal of Mathematics*, vol. 2021, Article ID 8634280, 9 pages, 2021.

[25] M. Awadalla, Y. Y. Yameni Noupoue, K. Abuasbeh, and G. Noureddine, "A fractional model approach for drug concentration in blood," Retrieved September 06, 2022, from https://assets.researchsquare.com/files/rs-1412567/v1_covered.pdf?c=1647012038.

[26] S. D. Undevia, G. Gomez-Abuin, and M. J. Ratain, "Pharmacokinetic variability of anticancer agents," *Nature Reviews Cancer*, vol. 5, no. 6, pp. 447–458, 2005.

[27] L.-E. Peyret, "Characteristics of anti-cancer drug adme - overview," OncologyPRO. (2015, July 16). Retrieved November 24, 2021, from https://oncologypro.esmo.org/oncology-in-practice/anti-cancer-agents-and-biological-therapy/drug-drug-interactions-with-kinase-inhibitors/general-introduction/characteristics-of-anti-cancer-drug-adme-overview.

[28] A. Tarek, "Ahmed pharmacokinetics of drugs following IV bolus, IV infusion, and oral administration," https://www.intechopen.com/chapters/49459.

[29] Chapter 2, "Chapter 2 - Page 8. (n.d.)," Retrieved May 21, 2022, from https://www.boomer.org/c/p4/c02/c0208.php.